species. This weakens the orbital overlap between the d_{yz} metal and p orbitals of the oxygen and as a consequence the antiferromagnetic coupling decreases in complexes **9** and **10** as compared to their μ-oxo counterparts.

Conclusion

We have developed an efficient synthetic route to oxo and hydroxo bridged, asymmetric, heterodinuclear complexes containing a ruthenium and a first-row transition-metal ion (V, Cr, Mn, Fe). The electronic properties of these complexes were found to be adequately described by using localized oxidation states for both metal ions. Depending on the propensity to form M=O bonds, the ruthenium ion adopts the +II, +III, or even +IV oxidation state. If both metal ions in a given complex have an odd number of d electrons, a very efficient antiferromagnetic superexchange pathway (S_{yz-yz}) couples the spins of the electrons at both metal ions. Protonation of the oxo bridge weakens this pathway significantly.

Acknowledgment. This work was supported by the Deutsche Forschungs-gemeinschaft and the Fonds der Chemischen Industrie. We thank both institutions.

Supplementary Material Available: Lists of atom coordinates, bond distances, bond angles, anisotropic displacement parameters, and calculated positional parameters for hydrogen atoms for complexes **4**, **6**, **7**, and **8** and listings of temperature-dependent susceptibilities of complexes (45 pages); listings of observed and calculated structure amplitudes (72). Ordering information is given on any current mashead page.

Zirconium and Hafnium Polyhydrides. 2. Preparation and Characterization of $M_3H_6(BH_4)_6(PMe_3)_4$ and $M_2H_4(BH_4)_4(dmpe)_2$

John E. Gozum, Scott R. Wilson, and Gregory S. Girolami*

Contribution from the School of Chemical Sciences, The University of Illinois at Urbana—Champaign, 505 South Mathews Avenue, Urbana, Illinois 61801.
Received March 18, 1992

Abstract: Prolonged treatment of the tetrakis(tetrahydroborate) complexes $Zr(BH_4)_4$ or $Hf(BH_4)_4$ with trimethylphosphine has given the first trinuclear group 4 polyhydrides, $M_3H_6(BH_4)_6(PMe_3)_4$, where M is Zr or Hf. The ^1H, ^{31}P, and ^{11}B NMR data suggest that these trinuclear compounds contain noncyclic $M(\mu\text{-}H)_3M(\mu\text{-}H)_3M$ backbones with the phosphine and tetrahydroborate ligands distributed in 2:2:0 and 2:1:3 ratios among the three metal centers. This suggestion has been confirmed by the X-ray crystal structure of $Zr_3H_6(BH_4)_6(PMe_3)_4$. The metal–metal vectors are each bridged by three hydride ligands: the average Zr–H–Zr angle is 108 (2)°, and the Zr···Zr···Zr angle is 124.14 (1)°. The Zr–B distances average 2.633 (4) Å for the η^2-BH_4 groups and 2.368 (6) Å for the η^3-BH_4 groups, while the Zr–P distances average 2.761 (1) Å. The average Zr···Zr distance is 3.164 (1) Å. Interestingly, several of the η^3-BH_4 groups are bonded asymmetrically, so that of the three Zr–H bonds to each BH_4 ligand, one Zr–H bond is longer than the other two. Addition of 1,2-bis(dimethylphosphino)ethane (dmpe) to the previously reported polyhydrides of stoichiometry $M_2H_3(BH_4)_5(PMe_3)_2$ results in phosphine exchange and loss of one BH_3 unit to yield the new dinuclear hydrides $M_2H_4(BH_4)_4(dmpe)_2$. The NMR and X-ray crystallographic data show that three of the hydrides bridge the Zr···Zr axis; the fourth hydride, one η^2-BH_4 group, and the two dmpe ligands are coordinated to one of the zirconium centers, while three asymmetrically-bonded η^3-BH_4 groups are coordinated to the other. The variable-temperature NMR data show that the terminal and bridging hydrides on zirconium exchange with each other via a "windshield wiper" type of motion with an activation energy of 12.6 ● 0.1 kcal mol^{-1}. The X-ray crystal structure of this molecule gives the following distances and angles: Zr···Zr = 3.150 (1) Å, Zr–H_b = 2.03 (8) Å, Zr–H_t = 1.74 (9) Å, Zr–P = 2.715 (3), 2.836 (3) Å, Zr–B = 2.70 (1) Å (η^2-BH_4), Zr–B = 2.39 (2) Å (η^3-BH_4), Zr–H–Zr = 107 (4)°. X-ray data for $C_{12}H_{66}B_6P_4Zr_3$ at 198 K: space group $P2_1/n$, a = 10.142 (5) Å, b = 18.499 (9) Å, c = 19.088 (8) Å, β = 90.49 (4)°, V = 3581 (5) Å^3, Z = 4, R_F = 0.022, and R_{wF} = 0.024 for 426 variables and 4000 unique data for which $I > 2.58\sigma(I)$. X-ray data for $C_{12}H_{52}B_4P_4Zr_2$ at 198 K: space group $Pna2_1$, a = 20.736 (4) Å, b = 9.894 (2) Å, c = 13.788 (4) Å, V = 2829 (2) Å^3, Z = 4, R_F = 0.046, and R_{wF} = 0.036 for 241 variables and 1965 unique data for which $I > 2.58\sigma(I)$.

Introduction

Compounds that contain direct metal–hydrogen bonds are of great interest due to the large number of stoichiometric and catalytic processes in which they are implicated.[1-3] Hydrides of the late transition metals are particularly active in these respects, and thus they have been studied extensively; in contrast, the chemistry of early transition metal hydrides remains largely unexplored, and polyhydrides of the early transition elements are particularly rare.[4-6] Although transition metal hydrides have traditionally been of interest due to their catalytic activity, they may also be involved in certain chemical vapor deposition processes for the growth of thin films that contain transition metals. Many CVD procedures employ H_2 as a carrier gas, and it is possible that in some cases transition metal hydrides are formed as intermediates that subsequently lose H_2 by reductive elimination.

(1) Muetterties, E. L. *Transition Metal Hydrides*; Marcel Dekker: New York, 1967.
(2) Bau, R. *Transition Metal Hydrides*, Advances in Chemistry Series 167; American Chemical Society: Washington, DC, 1978.
(3) Kaesz, H. D.; Saillant, R. B. *Chem. Rev.* **1972**, *72*, 231-281.
(4) Toogood, G. E.; Wallbridge, M. G. H. *Adv. Inorg. Chem. Radiochem.* **1982**, *25*, 267-340.
(5) For Part 1 of this series, see: Gozum, J. E.; Girolami, G. S. *J. Am. Chem. Soc.* **1991**, *113*, 3829-3837.
(6) For the present discussion, polyhydrides will be defined as coordination complexes that contain more than one hydride per metal center.

0002-7863/92/1514-9483$03.00/0

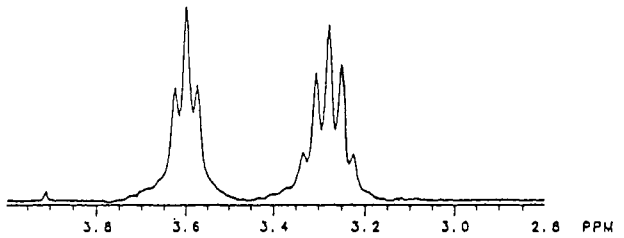

Figure 1. 500-MHz ^1H NMR spectrum of $Zr_3H_6(BH_4)_6(PMe_3)_4$, **1**, in C_7D_8 at −80 °C. Only the hydride resonances are shown.

Early transition metal tetrahydroborates such as $Zr(BH_4)_4$ and $Hf(BH_4)_4$ have been shown in recent years to serve as CVD precursors to metal diboride phases at deposition temperatures as low as 250 °C.[7-13] In this process, the boron-to-metal ratio changes from 4:1 in the precursor to 2:1 in the final film, and diborane and hydrogen are evolved as byproducts. Transition metal hydrides may be involved as intermediates during film growth; in a formal sense the conversion of precursor to product may be written

$$M(BH_4)_4 \xrightarrow{-B_2H_6} \text{“}MH_2(BH_4)_2\text{”} \xrightarrow{-5H_2} MB_2$$

In order to ascertain whether zirconium and hafnium hydrides are chemically reasonable intermediates in the conversion of these precursors to ZrB_2 and HfB_2, we have been studying the reactions of $Zr(BH_4)_4$ and $Hf(BH_4)_4$ with Lewis bases. We have recently reported the isolation of several polyhydrides of Zr and Hf by this method; among these were the mononuclear hydrides $MH(BH_4)_3(dmpe)$ and $MH_2(BH_4)_2(dmpe)_2$ and the dinuclear polyhydrides $M_2H_3(BH_4)_5(PMe_3)_2$.[5] We now describe the preparation of four new group 4 polyhydrides with boron-to-metal ratios of 2:1. The new complexes are polynuclear and have stoichiometries of $[MH_2(BH_4)_2]_2L_x$ and $[MH_2(BH_4)_2]_3L_x$; these species are accordingly the first Lewis base stabilized oligomers of the “$MH_2(BH_4)_2$” fragment for M = Zr or Hf.

Results

Preparation of Trinuclear Polyhydrides. Treatment of $Zr(BH_4)_4$ with 4.5 equiv of PMe_3 in diethyl ether at 25 °C for 5 h followed by removal of the solvent and crystallization from toluene affords colorless crystals of the trinuclear polyhydride $Zr_3H_6(BH_4)_6(PMe_3)_4$, **1**; this compound is obtained from the same solutions that yield the previously described dinuclear species $Zr_2H_3(BH_4)_5(PMe_3)_2$[5] except that a longer reaction time is employed (see Figure 4 below for a diagram of the structure of the previously reported dinuclear complex $Zr_2H_3(BH_4)_5(PMe_3)_2$). The analogous hafnium complex **2** may be prepared similarly. Interestingly, the colorless zirconium compound is obtained from burgundy-colored solutions; these solutions may contain a lower-valent zirconium compound that is also formed under the reaction conditions. To date, however, we have not been able to isolate this burgundy-colored compound from its solutions.

$$3M(BH_4)_4 + 10PMe_3 \rightarrow M_3H_6(BH_4)_6(PMe_3)_4 + 6PMe_3{\cdot}BH_3$$
$$\mathbf{1}: M = Zr \qquad \mathbf{2}: M = Hf$$

Table I. NMR Data for the New Zirconium and Hafnium Polyhydride Complexes[a]

	$Zr_3H_6(BH_4)_6(PMe_3)_4$, **1**	$Hf_3H_6(BH_4)_6(PMe_3)_4$, **2**
	^1H NMR, −80 °C	
MH	3.28 (quintet, J_{PH} = 14)	7.99 (quintet, J_{PH} = 14)
	3.60 (t, J_{PH} = 13)	8.24 (t, J_{PH} = 13)
$M(BH_4)$	2.10 (br s)	3.23 (br s)
$M(PMe_3)_2$	0.90 (d, J_{PH} = 8)	0.97 (d, J_{PH} = 8)
	1.23 (d, J_{PH} = 8)	1.26 (d, J_{PH} = 8)
	1.27 (s)	1.32 (s)
	^1H NMR, 20 °C	
MH	3.38 (q, J_{HH} = 1)	8.21 (s)
	3.60 (q, J_{HH} = 1)	8.29 (s)
$M(BH_4)$	1.85 (br q, J_{BH} = 81)	3.00 (br q, J_{BH} = 81)
$M(PMe_3)_2$	1.29 (d, J_{PH} = 3)	1.27 (s)
	$^{11}B\{^1H\}$ NMR, 20 °C	
$M(BH_4)_1$	−20.9 (s)	−22.7 (s)
$M(BH_4)_3$	−14.0 (s)	−15.4 (s)
$M(BH_4)_2$	−10.4 (s)	−12.4 (s)
	$^{31}P\{^1H\}$ NMR, −80 °C	
MP_A	−19.6 (s)[b]	−10.7 (s)[c]
MP_B	−20.3 (d)[b]	−12.3 (d)[c]
MP_C	−22.2 (d)[b]	−15.1 (d)[c]
	$^{31}P\{^1H\}$ NMR, 20 °C	
$MPMe_3$	−21.4 (s)	−14.2 (s)
	$Zr_2H_4(BH_4)_4(dmpe)_2$, **3**	$Hf_2H_4(BH_4)_4(dmpe)_2$, **4**
	^1H NMR, −80 °C	
MH_b	*d*	5.18 (s)
MH_t	5.35 (tt, J_{PH} = 75, 11)	8.39 (tt, J_{PH} = 61, 10)
$M(BH_4)$	−0.91 (s, br)	−0.52 (s, br)
$M(BH_4)_3$	1.96 (s, br)	3.02 (s, br)
PMe_2	0.76 (d, J_{PH} = 5)	0.83 (d, J_{PH} = 5)
PMe_2	1.25 (d, J_{PH} = 5)	1.30 (d, J_{PH} = 5)
PCH_2	1.31 (s)	1.41 (s)
PCH_2	1.44 (s)	1.50 (s)
	^1H NMR, 40 °C	
MH	2.99 (br)	5.98 (br)
$M(BH_4)$	−1.10 (q, J_{BH} = 83)	−0.68 (q, J_{BH} = 83)
$M(BH_4)_3$	1.26 (q, J_{BH} = 86)	2.75 (q, J_{BH} = 84)
PMe_2	1.10 (s)	1.18 (s)
PMe_2	1.25 (s)	1.43 (s)
PCH_2	1.37 (s)	1.59 (s)
	$^{11}B\{^1H\}$ NMR, 20 °C	
$M(BH_4)_3$	−15.1 (s)	−16.2 (s)
$M(BH_4)$	−33.1 (s)	−35.3 (s)
	$^{31}P\{^1H\}$ NMR, −80 °C	
MP_A	−6.5 (t, “J_{PP}” = 22)[e]	−5.1 (t, “J_{PP}” = 24)[e]
MP_B	11.4 (t, “J_{PP}” = 22)[e]	13.0 (t, “J_{PP}” = 24)[e]
	$^{31}P\{^1H\}$ NMR, 20 °C	
MP_A	−6.9 (s)	−4.6 (s)
MP_B	11.3 (s)	12.7 (s)

[a] Coupling constants in Hz. [b] A_2BC spin system, J_{BC} = 47, J_{AB} = J_{AC} = 0. [c] A_2BC spin system, J_{BC} = 39, J_{AB} = J_{AC} = 0. [d] Obscured by BH_4 and dmpe resonances. Chemical shift appears to be near δ 2.20. [e] “Deceptively simple” AA′BB′ spin system.

The infrared spectra of **1** and **2** contain strong bands in the 2000–2600-cm^{-1} region that suggest the presence of both bidentate and tridentate BH_4^- groups. However, absorptions due to the hydride ligands are not readily apparent. The hydride ligands all bridge between the metal centers (see below), and the metal–hydride stretching modes are probably obscured by C–H and B–H bending vibrations near 1500 cm^{-1}. Clearly identifiable infrared bands attributable to the hydride ligands were also absent in the spectra of the analogous dinuclear complexes $M_2H_3(BH_4)_5(PMe_3)_2$.[5]

The trinuclear nature of the compounds and details of their structures have been established by NMR spectroscopy (Table I). The ^1H NMR spectrum of **1** in d toluene-d_8 at −80 °C shows

(7) Jensen, J. A.; Gozum, J. E.; Pollina, D. M.; Girolami, G. S. *J. Am. Chem. Soc.* **1988**, *110*, 1643–1644.
(8) Girolami, G. S.; Jensen, J. A.; Gozum, J. E.; Pollina, D. M. *Mater. Res. Soc. Symp. Proc.* **1988**, *121*, 429–438.
(9) Jensen, J. A.; Gozum, J. E.; Rogers, D. M.; Girolami, G. S. Manuscript in preparation.
(10) Wayda, A. L.; Schneemeyer, L. F.; Opila, R. L. *Appl. Phys. Lett.* **1988**, *53*, 361–363.
(11) Rice, G. W.; Woodlin, R. L. *J. Am. Ceram. Soc.* **1988**, *71*, C181–C183.
(12) Baker, R. T.; Tebbe, F. N. 198th National Meeting of the American Chemical Society, Miami, FL, 1989; INOR 199.
(13) Gallagher, M. K.; Rhine, W. E.; Bowen, H. K. *Proceedings 3rd International Conference on Ultrastructure and Processing of Ceramics, Glasses, and Composites*, 1987.

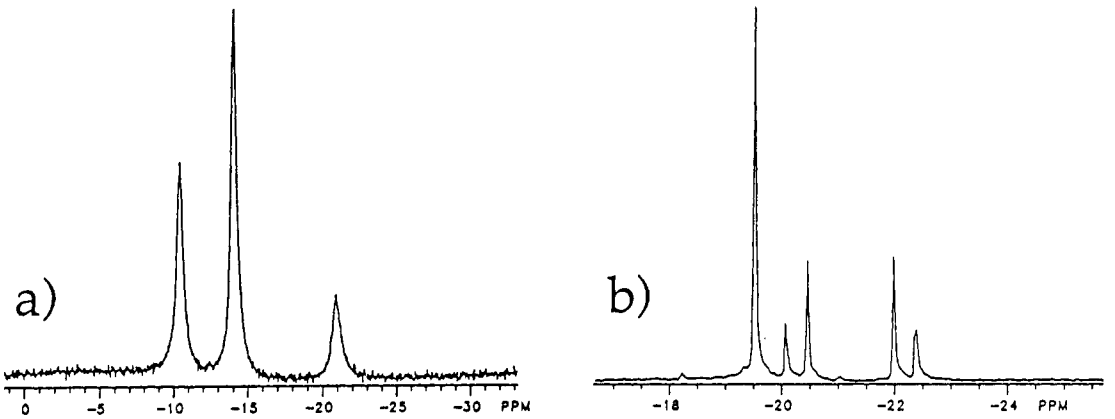

Figure 2. Heteronuclear NMR spectra of $Zr_3H_6(BH_4)_6(PMe_3)_4$, **1**, in C_7D_8: (a) 96.3-MHz $^{11}B\{^1H\}$ NMR spectrum at 20 °C and (b) 121.5-MHz $^{31}P\{^1H\}$ NMR spectrum at −80 °C.

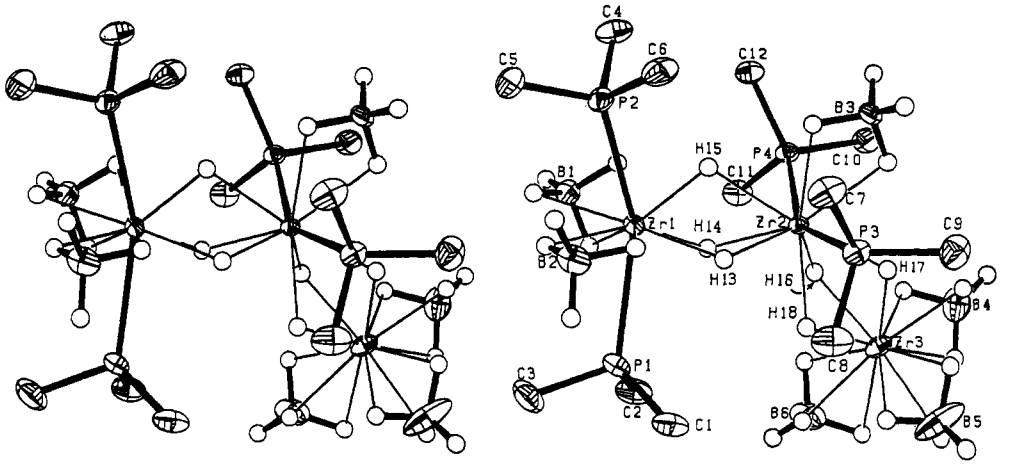

Figure 3. Stereoview of the molecular structure of $Zr_3H_6(BH_4)_6(PMe_3)_4$, **1**, showing the 35% probability surfaces. The hydrogen atoms are represented by arbitrarily-sized spheres.

the presence of two hydride environments: a triplet at δ 3.58 which is coupled to two phosphine ligands, and a quintet at δ 3.28 which is coupled to four phosphine ligands (Figure 1). The $^{11}B\{^1H\}$ NMR spectrum at 20 °C shows three singlets at δ −10.4, −14.0, and −20.9 whose relative intensities are 2:3:1, respectively (Figure 2a). The $^{31}P\{^1H\}$ NMR spectrum at −80 °C shows a singlet of intensity two at δ_A = −19.6 and doublets at δ_B = −20.3 and δ_C = −22.2, with J_{BC} = 47 Hz (Figure 2b). The spectrum corresponds to an A_2BC spin system where $J_{AB} = J_{AC} = 0$. Similar NMR parameters are observed for the hafnium analogue except that J_{BC} = 39 Hz.

The NMR data are consistent with a noncyclic trinuclear structure in which the metal centers and the hydride ligands form a $M(\mu\text{-}H)_3M(\mu\text{-}H)_3M$ backbone. If the phosphine and tetrahydroborate groups are distributed in 2:2:0 and 2:1:3 ratios among the three metal centers, then the NMR data can be rationalized. Specifically, the hydrides are involved in two-bond $^2J_{PH}$ couplings of ca. 13 Hz with the ^{31}P nuclei of the PMe_3 ligands, and thus a quintet and a triplet are seen. In addition, the A_2BC spin system in the $^{31}P\{^1H\}$ NMR spectrum can be accounted for as well: the two PMe_3 groups on the central metal center are chemically equivalent, but the two PMe_3 groups on the end metal center are not (see below). The latter two phosphines are more-or-less trans to one another and are coupled by a $^2J_{PP}$ coupling constant of ca. 40 Hz.

Molecular Structure of $Zr_3H_6(BH_4)_6(PMe_3)_4$. Single crystals of $Zr_3H_6(BH_4)_6(PMe_3)_4$ were grown from toluene and crystallize in the monoclinic space group $P2_1/n$ with one molecule in the asymmetric unit. Each molecule resides on a general position. Crystal data are given in Table II, while final bond distances and angles are given in Tables III and IV.

The structural analysis confirms that crystals of **1** are composed of discrete trinuclear molecules of stoichiometry $Zr_3H_6(BH_4)_6(PMe_3)_4$ (Figure 3). The three zirconium atoms are arranged in a nonlinear fashion in which the Zr···Zr···Zr angle is 124.14 (1)°, and each Zr–Zr vector is bridged by three bridging hydrides which were located in the X-ray difference maps and refined. The

Table II. Crystallographic Data for $Zr_3H_6(BH_4)_6(PMe_3)_4$ (**1**) and $Zr_2H_4(BH_4)_4(dmpe)_2$ (**3**)

	1	**3**
space group	$P2_1/n$	$Pna2_1$
T, °C	−75	−75
a, Å	10.142 (5)	20.736 (4)
b, Å	18.499 (9)	9.894 (2)
c, Å	19.088 (8)	13.788 (4)
β, °	90.49 (4)	90
V, Å^3	3581 (5)	2829 (2)
Z	4	4
mol wt	673.08	546.12
d_{calcd}, g cm^{-3}	1.248	1.282
μ_{calcd}, cm^{-1}	10.21	9.45
size, mm	0.2 × 0.3 × 0.5	0.1 × 0.2 × 0.2
diffractometer	Enraf-Nonius CAD4	
radiation	Mo K$\bar{\alpha}$, $\bar{\lambda}$ = 0.71073 Å	
monochromator	graphite crystal, 2θ = 12°	
scan range, type	$2.0 \le 2\theta < 54°$, ω/θ	
scan speed	3–16 deg min^{-1}	
scan width	$\Delta\omega$ (deg) = 1.50[1.00 + 0.35 tan θ]	
rflctns, total	5600	4203
rflctns, unique	4956	3246
rflctns, $I > 2.58\sigma(I)$	4000	1965
R_i	0.020	0.016
R_F	0.022	0.046
R_{wF}	0.024	0.036
variables	426	241
p factor	0.010	0.010

Table III. Selected Bond Distances (Å) and Angles (deg) for the Non-Hydrogen Atoms in $Zr_3H_6(BH_4)_6(PMe_3)_4$, **1**

Bond Distances			
Zr(1)···Zr(2)	3.176 (1)	Zr(2)–P(3)	2.766 (1)
Zr(1)–P(1)	2.758 (1)	Zr(2)–P(4)	2.765 (1)
Zr(1)–P(2)	2.755 (1)	Zr(2)–B(3)	2.655 (4)
Zr(1)–B(1)	2.352 (4)	Zr(3)–B(4)	2.363 (6)
Zr(1)–B(2)	2.610 (4)	Zr(3)–B(5)	2.361 (6)
Zr(2)···Zr(3)	3.152 (1)	Zr(3)–B(6)	2.394 (6)
Bond Angles			
P(1)–Zr(1)–P(2)	152.45 (3)	Zr(2)–Zr(1)–B(2)	121.7 (1)
P(3)–Zr(2)–P(4)	152.61 (3)	Zr(1)–Zr(2)–Zr(3)	124.14 (1)
B(1)–Zr(1)–B(2)	122.3 (1)	Zr(1)–Zr(2)–P(3)	101.77 (2)
B(4)–Zr(2)–B(5)	106.2 (2)	Zr(1)–Zr(2)–P(4)	94.45 (2)
B(4)–Zr(2)–B(6)	105.1 (2)	Zr(1)–Zr(2)–B(3)	117.5 (1)
B(5)–Zr(2)–B(6)	106.6 (2)	Zr(2)–Zr(3)–B(4)	110.0 (1)
Zr(2)–Zr(1)–P(1)	96.31 (2)	Zr(2)–Zr(3)–B(5)	114.1 (2)
Zr(2)–Zr(1)–P(2)	105.69 (2)	Zr(2)–Zr(3)–B(6)	114.2 (1)
Zr(2)–Zr(1)–B(1)	116.0 (1)		

Table IV. Selected Bond Distances (Å) and Angles (deg) for the Hydrogen Atoms in $Zr_3H_6(BH_4)_6(PMe_3)_4$, **1**

Bond Distances			
Zr(1)–H(13)	1.93 (3)	B(1)–H(B1a)	1.17 (4)
Zr(1)–H(14)	1.95 (3)	B(1)–H(B1b)	1.18 (4)
Zr(1)–H(15)	1.83 (3)	B(1)–H(B1c)	1.19 (3)
Zr(2)–H(13)	1.94 (3)	B(1)–H(B1d)	1.03 (4)
Zr(2)–H(14)	1.98 (3)	B(2)–H(B2a)	1.14 (4)
Zr(2)–H(15)	2.13 (3)	B(2)–H(B2b)	1.14 (4)
Zr(2)–H(16)	1.94 (3)	B(2)–H(B2c)	1.09 (4)
Zr(2)–H(17)	1.93 (3)	B(2)–H(B2d)	1.08 (4)
Zr(2)–H(18)	2.00 (4)	B(3)–H(B3a)	1.14 (4)
Zr(3)–H(16)	1.96 (3)	B(3)–H(B3b)	1.13 (4)
Zr(3)–H(17)	1.88 (3)	B(3)–H(B3c)	1.08 (4)
Zr(3)–H(18)	1.95 (3)	B(3)–H(B3d)	1.03 (4)
Zr(1)–H(B1a)	2.05 (3)	B(4)–H(B4a)	1.21 (4)
Zr(1)–H(B1b)	2.11 (4)	B(4)–H(B4b)	1.10 (4)
Zr(1)–H(B1c)	2.21 (3)	B(4)–H(B4c)	1.14 (4)
Zr(1)–H(B2a)	2.14 (3)	B(4)–H(B4d)	1.11 (4)
Zr(1)–H(B2b)	2.15 (4)	B(5)–H(B5a)	1.08 (4)
Zr(2)–H(B3a)	2.19 (3)	B(5)–H(B5b)	1.03 (4)
Zr(2)–H(B3b)	2.12 (4)	B(5)–H(B5c)	1.19 (4)
Zr(3)–H(B4a)	2.08 (3)	B(5)–H(B5d)	1.02 (4)
Zr(3)–H(B4b)	2.24 (3)	B(6)–H(B6a)	1.14 (4)
Zr(3)–H(B4c)	2.08 (3)	B(6)–H(B6b)	1.12 (4)
Zr(3)–H(B5a)	2.06 (4)	B(6)–H(B6c)	1.14 (4)
Zr(3)–H(B5b)	2.10 (4)	B(6)–H(B6d)	0.98 (4)
Zr(3)–H(B5c)	2.19 (4)		
Zr(3)–H(B6a)	2.35 (4)		
Zr(3)–H(B6b)	2.19 (3)		
Zr(3)–H(B6c)	2.11 (4)		
Bond Angles			
Zr(1)–H(13)–Zr(2)	110 (2)	H(13)–Zr(2)–H(14)	60 (1)
Zr(1)–H(14)–Zr(2)	108 (2)	H(13)–Zr(2)–H(15)	57 (1)
Zr(1)–H(15)–Zr(2)	107 (2)	H(14)–Zr(2)–H(15)	60 (1)
Zr(2)–H(16)–Zr(3)	108 (2)	H(16)–Zr(2)–H(17)	62 (1)
Zr(2)–H(17)–Zr(3)	111 (2)	H(16)–Zr(2)–H(18)	60 (1)
Zr(2)–H(18)–Zr(3)	106 (1)	H(17)–Zr(2)–H(18)	59 (1)
H(13)–Zr(1)–H(14)	60 (1)	H(16)–Zr(3)–H(17)	63 (1)
H(13)–Zr(1)–H(15)	62 (1)	H(16)–Zr(3)–H(18)	60 (1)
H(14)–Zr(1)–H(15)	66 (1)	H(17)–Zr(3)–H(18)	60 (1)

phosphine and tetrahydroborate ligands in this trinuclear molecule are distributed unequally among the three zirconium atoms. The zirconium atom at one end of the trinuclear unit, Zr(3), is coordinated to three tridentate tetrahydroborate ligands; the central zirconium, Zr(2), is ligated by one bidentate BH_4^- group, and the third zirconium center, Zr(1), possesses one bidentate and one tridentate BH_4^- ligand. The latter two zirconium centers are each coordinated to two mutually trans PMe_3 ligands as well. The four phosphine ligands are staggered with respect to the Zr(1)–Zr(2) axis, presumably to minimize steric repulsions between these groups. The Zr(1)···Zr(2) distance of 3.176 (1) Å is slightly longer than the Zr(2)···Zr(3) distance of 3.152 (1) Å; neither of these Zr···Zr contact distances in **1** is indicative of a direct Zr–Zr bonding interaction, but instead they both are dictated by the constraints imposed by the hydride bridges.

The coordination numbers of all of the zirconium centers are high and the coordination polyhedra are difficult to describe if each individual Zr–H contact is included. However, if one considers the BH_4^- groups to occupy one coordination site each and the three bridging hydrides collectively to occupy another coordination site, then the coordination polyhedra about each zirconium center may be described more conveniently. The two phosphine-ligated zirconium atoms, Zr(1) and Zr(2), adopt trigonal-bipyramidal geometries with the two PMe_3 ligands on each center occupying the axial positions; the third zirconium atom, Zr(3), adopts a tetrahedral geometry. Alternatively, since all three BH_4^- ligands on Zr(3) are approximately trans to one of the three bridging hydride ligands that connect this center to Zr(2), the coordination geometry about Zr(3) may also be described as fac-octahedral.

A comparison of the previously reported dinuclear hydride $Zr_2H_3(BH_4)_5(PMe_3)_2$[5] and the present trinuclear compound suggests that the latter molecule is slightly more crowded sterically. Thus, the average Zr–P distance of 2.750 (1) Å in $Zr_2H_3(BH_4)_5(PMe_3)_2$ is somewhat shorter than the 2.761 (1) Å average Zr–P distance in $Zr_3H_6(BH_4)_6(BH_4)_6(PMe_3)_4$. Similarly, the Zr···Zr distance in the dinuclear complex measures 3.124 (1) Å while the Zr···Zr distances in the trinuclear complex are slightly longer at 3.152 (1) and 3.176(1) Å. Furthermore, the longest Zr···Zr distance in $Zr_3H_6(BH_4)_6(PMe_3)_4$ occurs between the two zirconium centers that are ligated by PMe_3, and this lengthening is presumably due to nonbonded repulsions between the ligands on these two sterically crowded centers. Finally, the Zr···B distances in $Zr_3H_6(BH_4)_6(PMe_3)_4$ are consistently ca. 0.02 Å longer than the equivalent distances in $Zr_2H_3(BH_4)_5(PMe_3)_2$. In all cases, steric congestion appears to be responsible for the relatively longer metal–metal and metal–ligand distances in $Zr_3H_6(BH_4)_6(PMe_3)_4$.

The hydrogen atom positions in $Zr_3H_6(BH_4)_6(PMe_3)_4$ are of interest, especially since they were readily apparent in the Fourier difference maps and their positions were determined relatively accurately (Table IV). The Zr–H_b distances to the bridging hydrides range from 1.83 (3) to 2.13 (3) Å and average 1.95 (3) Å. The differences among the individual Zr–H_b distances are not statistically significant, and thus within experimental error the hydride ligands all bridge symmetrically. The 1.95 (3) Å average Zr–H_b distance is very similar to the 1.92 (4) Å average in $Zr_2H_3(BH_4)_5(PMe_3)_2$.[5] The average Zr–H_b–Zr angle of 107° is also similar to the 110° average for these angles in $Zr_2H_3(BH_4)_5(PMe_3)_2$.

The BH_4^- groups show the expected variations in B–H distances: the average B–H distance of 1.14 (4) Å to the hydrogen atoms that bridge to zirconium is longer than the average B–H distance of 1.05 (4) Å to the hydrogen atoms that are terminal on boron.

Close examination of the tetrahydroborate ligands on Zr(3) reveals that, in each of three η^3-BH_4^- groups, one of the Zr(3)–H distances is longer than the other two. Specifically, the long Zr(3)–H distances average 2.26 (4) Å, while the short Zr(3)–H distances average 2.10 (4) Å. Although this difference is of marginal significance statistically, in each case the long Zr–H bond to the BH_4^- groups is approximately trans to one of the hydrides that bridges the Zr(2)···Zr(3) axis. (The relevant angles, H(16)–Zr(3)–H(B5c), H(17)–Zr(3)–H(B6a), and H(18)–Zr(3)–H(B4b), are all 175 (1)°.) As a result of this trans influence, the three tetrahydroborate groups on Zr(3) are coordinated in a fashion that is intermediate between η^2-BH_4^- and η^3-BH_4^- coordination modes. We are not aware of any other transition metal tetrahydroborate complexes that contain similarly bonded BH_4^- ligands.

Trinuclear zirconium and hafnium hydride complexes have not been previously described, although one heteronuclear complex $Cp_6Y_2ZrH_4$ is known.[14] A tetranuclear hafnium complex, $[Cp^*HfH_2Cl]_4$, has also been synthesized recently.[15] Asymmetric

(14) Evans, W. J.; Meadows, J. H.; Hanusa, T. P. *J. Am. Chem. Soc.* **1984**, *106*, 4454–4460.

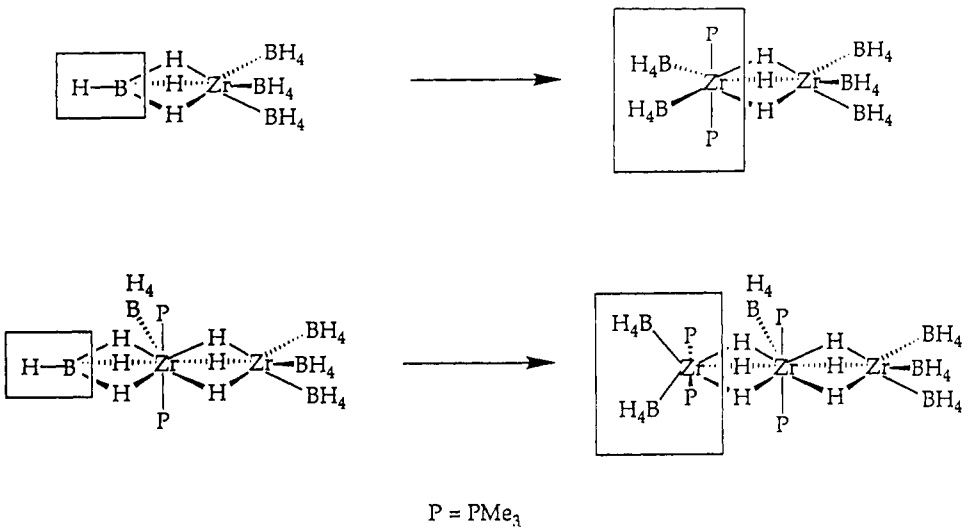

Figure 4. Structural relationship between zirconium hydrides. Successive replacement of $[BH^{2+}]$ units by $[Zr(BH_4)_2(PMe_3)_2^{2+}]$ units gives the series $Zr(BH_4)_4 \rightarrow Zr_2H_3(BH_4)_5(PMe_3)_2 \rightarrow Zr_3H_6(BH_4)_6(PMe_3)_4$.

distributions of ligands in polynuclear phosphine/polyhydride complexes are uncommon, but have been observed in species such as $[Re_2H_9(Ph_2PCH_2)_3CMe^-]$,[16] $Re_2H_6(PMe_2Ph)_5$,[17] $Re_2H_4(PMe_2Ph)_4(P(OCH_2)_3CEt)_2$,[18] $Rh_2H_4[P(NMe_2)_3]_4$,[19] and $[Pt_2H_3(PEt_3)_4^+]$,[20] besides the group 4 complexes discussed in our earlier paper.[5,21]

Structural Relationships between Zirconium Polyhydrides. The structure of $Zr_3H_6(BH_4)_6(PMe_3)_4$ and that of the previously reported dinuclear complex $Zr_2H_3(BH_4)_5(PMe_3)_2$ are unexpectedly asymmetric, but in fact their structures are closely related not only to each other but also to that of the starting material $Zr(BH_4)_4$. If one $B-H^{2+}$ unit of one of the tridentate BH_4^- groups in the starting material $Zr(BH_4)_4$[22,23] is replaced with a charge equivalent $[Zr(BH_4)_2(PMe_3)_2^{2+}]$ fragment, the dinuclear species $Zr_2H_3(BH_4)_5(PMe_3)_2$ is generated (Figure 4). If one again replaces a $B-H^{2+}$ of one of the tridentate tetrahydroborate groups in $Zr_2H_3(BH_4)_5(PMe_3)_2$ with a second $[Zr(BH_4)_2(PMe_3)_2^{2+}]$ group, the result is the trizirconium species $Zr_3H_6(BH_4)_6(PMe_3)_4$. While this replacement process is almost certainly not the mechanism by which these molecules are generated, it nonetheless serves to emphasize that these molecules are closely related structurally.

Interestingly, the observed structure of $Zr_3H_6(BH_4)_6(PMe_3)_4$ is not the only isomer possible given this stoichiometry. Specifically, a more symmetric trinuclear structure would result if a $B-H^{2+}$ unit of one of the three tetrahydroborate groups of the $Zr(BH_4)_3$ center in $Zr_2H_3(BH_4)_5(PMe_3)_2$ were replaced with a $[Zr(BH_4)_2(PMe_3)_2^{2+}]$ fragment. The resulting trinuclear molecule would have a symmetric $[Zr(BH_4)_2(PMe_3)_2]H_3[Zr(BH_4)_2]H_3[Zr(BH_4)_2(PMe_3)_2]$ structure. It is not entirely clear whether the isomer isolated is formed under kinetic or thermodynamic control.

It is interesting to consider whether longer chains of zirconium centers can be synthesized by successive formal replacement of $B-H^{2+}$ units with $[Zr(BH_4)_2(PMe_3)_2^{2+}]$ fragments. We have not been able to prepare such longer-chain polynuclear zirconium hydrides to date. In fact, molecular models suggest that there is not enough room for the PMe_3 groups if the chain is extended to four zirconium centers: this is a consequence of the bent nature of the Zr backbone of the molecules, in which the Zr···Zr···Zr angles are approximately 124°. If one starts with the structure of $Zr_3H_6(BH_4)_6(PMe_3)_4$ and replaces a $B-H^{2+}$ unit of a BH_4^- group on Zr(3) with another $Zr(BH_4)_2(PMe_3)_2$ center whose PMe_3 ligands are staggered with respect to the PMe_3 groups on Zr(3), unacceptably short contacts between the phosphines on Zr(2) and the fourth zirconium center result. Thus, a trinuclear molecule appears to be the largest of this class that is allowed sterically.

Dynamic Behavior of the $M_3H_6(BH_4)_6(PMe_3)_4$ Complexes. Although the variable-temperature NMR spectra of $Zr_3H_6(BH_4)_6(PMe_3)_4$ and $Hf_3H_6(BH_4)_6(PMe_3)_4$ show no direct evidence of dynamic behavior, the simplicity of the NMR spectra is not consistent with the asymmetric structures of these complexes unless dynamic processes are occurring. Specifically, there must be an exchange process that interconverts the η^2-BH_4^- and η^3-BH_4^- groups on Zr(1) since these two ligands are chemically equivalent in the ^1H and ^{11}B NMR spectra, but chemically inequivalent in the solid-state structure. A second exchange process is necessary to interconvert the three tridentate BH_4^- groups on Zr(3), since these are also chemically inequivalent in the static structure. Finally, an exchange process is necessary to give only two hydride environments instead of six. Rotational motions about the Zr(1)···Zr(2) and Zr(2)···Zr(3) axes would be sufficient to exchange the hydrides and the three η^3-BH_4 groups on Zr(3). All of these dynamic processes are similar to those that operate in the structurally related $M_2H_3(BH_4)_5(PMe_3)_2$ dinuclear hydrides described previously.[5] Interestingly, the BH_4^- groups on Zr(1), Zr(2), and Zr(3) do not exchange with each other. This finding is also consistent with the behavior of the $M_2H_3(BH_4)_5(PMe_3)_2$ complexes.

At elevated temperatures (50 °C), reversible PMe_3 dissociation becomes fast on the NMR time scale, as judged by the loss of P–H coupling with the bridging hydrides. Under these conditions, a J_{HH} coupling of 1 Hz between the two sets of three bridging hydrides becomes observable. This H–H coupling is much smaller than the J_{HH} coupling of 7.5 Hz between the terminal and bridging hydrides in $[Cp'_2ZrH_2]_2$.[24]

Reaction of $M_2H_3(BH_4)_5(PMe_3)_2$ with Bidentate Phosphines. We have previously shown that the reaction of trimethylphosphine with zirconium or hafnium tetrahydroborates produces dinuclear species with bridging hydride ligands of stoichiometry $M_2H_3(BH_4)_5(PMe_3)_2$.[5] We were interested to determine whether more hydride-rich stoichiometries could be obtained by further reactions

(15) Booij, M.; Blenkers, J.; Sinnema, J. C. M.; Meetsma, A.; van Bolhuis, F.; Teuben, J. H. *Organometallics* **1988**, *7*, 1029–1032.
(16) Abrahams, S. C.; Ginsberg, A. P.; Koetzle, T. F.; Marsh, P.; Sprinkle, C. R. *Inorg. Chem.* **1986**, *25*, 2500–2510.
(17) Green, M. A.; Huffman, J. C.; Caulton, K. G. *J. Am. Chem. Soc.* **1981**, *103*, 695–696.
(18) Green, M. A.; Huffman, J. C.; Caulton, K. G. *J. Am. Chem. Soc.* **1982**, *104*, 2319–2320.
(19) Meier, E. B.; Burch, R. R.; Muetterties, E. L.; Day, V. W. *J. Am. Chem. Soc.* **1982**, *104*, 2661–2663.
(20) Bracher, G.; Grove, D. M.; Pregosin, P. S.; Venanzi, L. M. *Angew. Chem., Int. Ed. Engl.* **1979**, *18*, 155–156.
(21) Fryzuk, M. D.; Rettig, S. J.; Westerhaus, A.; Williams, H. D. *Inorg. Chem.* **1985**, *24*, 4316–4325.
(22) Plato, V.; Hedberg, K. *Inorg. Chem.* **1971**, *10*, 590–594.
(23) For the structure of $Hf(BH_4)_4$, see: Broach, R. W.; Chuang, I.-S.; Marks, T. J.; Williams, J. W. *Inorg. Chem.* **1983**, *22*, 1081–1084.
(24) Jones, S. B.; Petersen, J. L. *Inorg. Chem.* **1981**, *20*, 2889–2894.

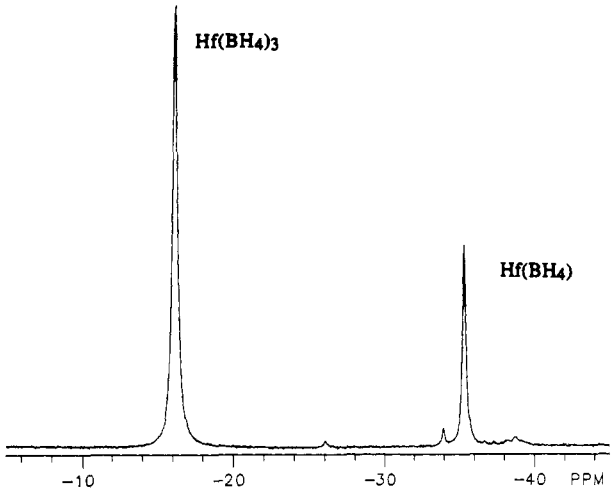

Figure 5. 96.3-MHz $^{11}B\{^1H\}$ NMR spectrum of $Hf_2H_4(BH_4)_4(dmpe)_2$, **4**, in C_7D_8 at 20 °C.

Table V. Selected Bond Distances (Å) and Angles (deg) for the Non-Hydrogen Atoms in $Zr_2H_4(BH_4)_4(dmpe)_2$, **3**

Bond Distances			
Zr(1)···Zr(2)	3.150 (1)	Zr(1)-B(1)	2.70 (1)
Zr(1)-P(1)	2.829 (3)	Zr(2)-B(2)	2.38 (2)
Zr(1)-P(2)	2.713 (3)	Zr(2)-B(3)	2.38 (2)
Zr(1)-P(3)	2.841 (3)	Zr(2)-B(4)	2.42 (2)
Zr(1)-P(4)	2.717 (3)		
Bond Angles			
P(1)-Zr(1)-P(2)	71.83 (9)	Zr(2)-Zr(1)-P(2)	101.34 (7)
P(1)-Zr(1)-P(3)	92.02 (9)	Zr(2)-Zr(1)-P(3)	93.93 (7)
P(2)-Zr(1)-P(4)	118.3 (1)	Zr(2)-Zr(1)-P(4)	102.79 (8)
P(3)-Zr(1)-P(4)	71.82 (9)	Zr(2)-Zr(1)-B(1)	178.4 (3)
B(2)-Zr(2)-B(3)	106.5 (6)	Zr(1)-Zr(2)-B(2)	115.4 (4)
B(2)-Zr(2)-B(4)	104.7 (5)	Zr(1)-Zr(2)-B(3)	114.6 (5)
B(3)-Zr(2)-B(4)	104.5 (6)	Zr(1)-Zr(2)-B(4)	110.0 (4)
Zr(2)-Zr(1)-P(1)	95.69 (7)		

of these dinuclear hydrides with bidentate phosphines such as 1,2-bis(dimethylphosphino)ethane (dmpe). Treatment of $Zr_2H_3(BH_4)_5(PMe_3)_2$ with 4 equiv of dmpe in pentane followed by removal of the solvent and crystallization from diethyl ether effects complete phosphine exchange and affords colorless crystals of the new zirconium hydride $Zr_2H_4(BH_4)_4(dmpe)_2$, **3**. The analogous hafnium complex **4** may be prepared similarly.

$$M_2H_3(BH_4)_5(PMe_3)_2 + 2dmpe \rightarrow M_2H_4(BH_4)_4(dmpe)_2 + PMe_3{\cdot}BH_3 + PMe_3$$

3: M = Zr
4: M = Hf

The infrared spectra again suggest the presence of both bidentate and tridentate BH_4^- ligands, but do not contain absorptions attributable to M-H stretches despite the presence of a terminal hydride ligand in both **3** and **4** (see below). Presumably, these peaks are also obscured by the C-H and B-H bending modes near 1500 cm^{-1}; similar behavior was noted for the related zirconium and hafnium terminal hydride complexes of stoichiometry $MH(BH_4)_3(dmpe)$ and $MH_2(BH_4)_2(dmpe)_2$.[5,35]

The ^1H NMR spectrum of **4** in toluene-d_8 at −80 °C shows the presence of two hydride environments: a broad singlet of intensity three at δ 5.18, and a triplet of triplets of intensity one at δ 8.39. The $^{11}B\{^1H\}$ NMR spectrum of **4** at 20 °C shows two singlets at δ −15.1 and −33.1 whose relative intensities are 3:1 (Figure 5). The $^{31}P\{^1H\}$ NMR spectrum at −80 °C shows two triplets at δ_A = 11.4 and δ_B = −6.5 that correspond to a "deceptively simple" AA'BB' spin system where J_{AB} = 21 Hz. Similar NMR parameters are observed for the zirconium analogue (Table I).

These NMR data are consistent with a binuclear structure in which the ligands are distributed as follows: $(BH_4)H(dmpe)_2M(\mu\text{-}H)_3M(BH_4)_3$. Both dmpe ligands are coordinated to one of the metal centers, a feature that is reminiscent of the asymmetric

Table VI. Selected Bond Distances (Å) and Angles (deg) for the Hydrogen Atoms in $Zr_2H_4(BH_4)_4(dmpe)_2$, **3**[a]

Bond Distances			
Zr(1)-H	1.74 (9)	B(1)-H(11)	1.09 (9)
Zr(1)-H(1)	2.00 (8)	B(1)-H(12)	1.09 (9)
Zr(1)-H(2)	1.99 (8)	B(1)-H(13)	1.21 (10)
Zr(1)-H(3)	2.10 (8)	B(1)-H(14)	1.06 (9)
Zr(2)-H(1)	1.86 (8)	B(2)-H(21)	1.09 (9)
Zr(2)-H(2)	1.82 (8)	B(2)-H(22)	1.00 (9)
Zr(2)-H(3)	2.01 (9)	B(2)-H(23)	1.32 (8)
Zr(1)-H(13)	2.32 (8)	B(2)-H(24)	0.98 (9)
Zr(1)-H(14)	2.33 (9)	B(3)-H(31)	0.98 (9)
Zr(2)-H(22)	2.25 (9)	B(3)-H(32)	0.94 (10)
Zr(2)-H(23)	2.22 (9)	B(3)-H(33)	1.22 (9)
Zr(2)-H(24)	2.28 (9)	B(3)-H(34)	1.14 (9)
Zr(2)-H(32)	2.13 (9)	B(4)-H(41)	0.96 (9)
Zr(2)-H(33)	2.22 (9)	B(4)-H(42)	1.25 (9)
Zr(2)-H(34)	2.35 (9)	B(4)-H(43)	1.38 (9)
Zr(2)-H(42)	2.23 (9)	B(4)-H(44)	1.18 (9)
Zr(2)-H(43)	2.08 (9)		
Zr(2)-H(44)	2.47 (9)		
Bond Angles			
Zr(1)-H(1)-Zr(2)	109 (4)	H(2)-Zr(1)-H(3)	60 (3)
Zr(1)-H(2)-Zr(2)	112 (4)	H(1)-Zr(2)-H(2)	63 (4)
Zr(1)-H(3)-Zr(2)	100 (4)	H(1)-Zr(2)-H(3)	65 (4)
H(1)-Zr(1)-H(2)	53 (3)	H(2)-Zr(2)-H(3)	65 (4)
H(1)-Zr(1)-H(3)	61 (3)	Zr(2)-Zr(1)-H	89 (3)

[a] For hydrogen atoms with two-digit indices, the first digit indicates the boron atom to which it is attached.

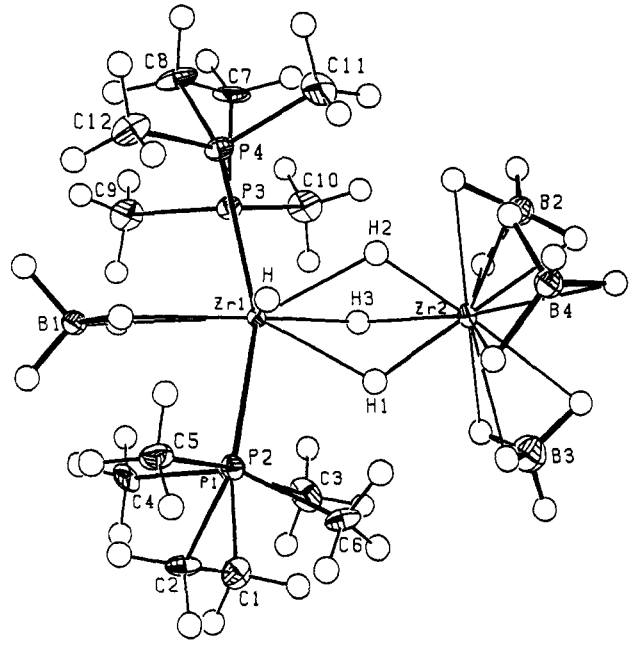

Figure 6. ORTEP diagram of the molecular structure of $Zr_2H_4(BH_4)_4(dmpe)_2$, **3**, showing the 35% probability surfaces. The hydrogen atoms are represented by arbitrarily-sized spheres. The terminal hydride ligand nearly eclipses Zr(1) in this view.

distribution of the PMe_3 ligands in the starting material $M_2H_3(BH_4)_5(PMe_3)_2$.[5] The reaction with dmpe has generated a fourth hydride ligand, which is terminally bound. All of these structural features have been confirmed by X-ray crystallography.

Molecular Structure of $Zr_2H_4(BH_4)_4(dmpe)_2$. Single crystals of $Zr_2H_4(BH_4)_4(dmpe)_2$ were grown by cooling saturated diethyl ether solutions to −20 °C and crystallized in the acentric orthorhombic space group $Pna2_1$ with one molecule in the asymmetric unit. Molecules of **3** reside on general positions in the unit cell. Crystal data for **3** are given in Table II, while final bond distances and angles are presented in Tables V and VI.

The X-ray crystal structure analysis shows that molecules of $Zr_2H_4(BH_4)_4(dmpe)_2$ contain two zirconium atoms connected by three bridging hydrides; the hydride ligands were located in the

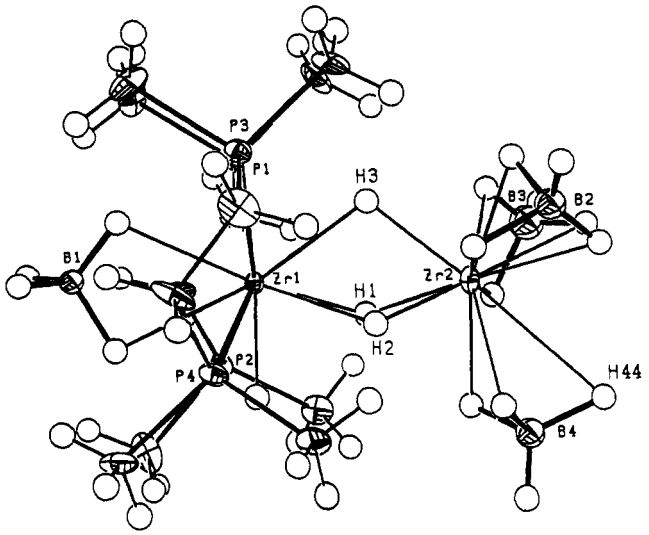

Figure 7. ORTEP diagram of $Zr_2H_4(BH_4)_4(dmpe)_2$, **3**, rotated 90° from the view in Figure 7, showing lengthening of the Zr(2)–H(44) bond.

X-ray difference map and their positions were independently refined (Figure 6). Once again, the ligands in this group 4 polyhydride are distributed asymmetrically among the zirconium atoms. Zirconium atom Zr(2) is surrounded by three tridentate tetrahydroborate ligands; the other zirconium center Zr(1) is ligated by two dmpe ligands, one BH_4^- group, and one terminal hydride ligand. The bidentate tetrahydroborate ligand on Zr(1) lies along an extension of the Zr(1)···Zr(2) axis, and the Zr–H_t vector to the terminal hydride ligand forms an angle of 90° with respect to this axis. The terminal hydride is approximately in the same plane as the two dmpe ligands. Overall, the geometry about Zr(1) is accordingly pentagonal bipyramidal, and that about Zr(2) is tetrahedral, if one follows the scheme discussed above for the structure of $Zr_3H_6(BH_4)_6(PMe_3)_4$.

The Zr(1)···Zr(2) distance of 3.150 (1) Å is within 0.025 Å of those in $Zr_2H_3(BH_4)_5(PMe_3)_2$ and $Zr_3H_6(BH_4)_6(PMe_3)_4$ (see above); the structure of the Zr(μ-H)$_3$Zr unit is therefore remarkably constant from compound to compound. The two bidentate phosphine ligands have two distinct Zr–P distances: the ends of the dmpe ligands closest to the terminal hydride (P2 and P4) average 2.708 (8) Å while those farthest from the hydride (P1 and P3) average 2.832 (3) Å. Presumably, the different Zr–P bond lengths minimize steric repulsions between these groups. The average Zr···B distances of 2.70 (1) Å to the bidentate BH_4^- group and 2.40 (2) Å to the tridentate BH_4^- groups are approximately 0.05 Å longer than those in $Zr_2H_3(BH_4)_5(PMe_3)_2$ and $Zr_3H_6(BH_4)_6(PMe_3)_4$.

The bridging hydrides are apparently arranged asymmetrically; the hydrides are only 1.87 (6) Å from the phosphine-free zirconium center, but are 2.04 (7) Å from the zirconium center that is coordinated to the sterically bulky dmpe ligands. This asymmetry, if real, is much more pronounced than in any of the other polynuclear group 4 hydrides we (or others) have prepared, and would be consistent with the *significantly* different electronic and steric natures of the two zirconium centers in **3**. The average Zr–H_b–Zr angle of 107 (4)° is typical of hydrides that bridge between group 4 metals.[5,24]

The terminal Zr–H_t distance is 1.74 (9) Å and as expected is shorter than all of the Zr–H_b distances; similar Zr–H_t contacts of 1.67, 1.78 (2), and 1.80 (5) Å have been observed in the molecules $(C_8H_{11})ZrH(dmpe)_2$,[25] $[Cp_2'ZrH_2]_2$,[24] and $CpZrH(C_4H_6)(dmpe)$.[26]

Inspection of the tetrahydroborate groups on Zr(2) again suggests that the η^3-BH_4^- groups on this center are distorted due to the trans influence of the hydrides that bridge to Zr(1). The distortion is most pronounced for the tetrahydroborate group centered on atom B(4) (Figure 7). This group is nearest the terminal hydride ligand on Zr(1) and exhibits two short Zr(2)–H distances of 2.08 (9) and 2.23 (9) Å and one longer Zr(2)–H distance of 2.47 (9) Å. As was seen in the structure of $Zr_3H_6(BH_4)_6(PMe_3)_4$ above, the long Zr–H bond is the one that is approximately trans to a bridging hydride ligand: the H(3)–Zr(2)–H(44) angle is 175 (1)°. Although of only marginal statistical significance, the distortions are occurring in a regular fashion that suggests they are in fact *chemically* significant.

A comparison of the structures of the trimethylphosphine complex $Zr_2H_3(BH_4)_5(PMe_3)_2$[5] and the dmpe-exchange product $Zr_2H_4(BH_4)_4(dmpe)_2$ is instructive. The Zr–P distances of 2.750 (1) Å for $Zr_2H_3(BH_4)_5(PMe_3)_2$ and 2.778 (1) Å for $Zr_2H_4(BH_4)_4(dmpe)_2$ suggest that the latter molecule is slightly more crowded. Similarly, the Zr···Zr distance and Zr···B distances are 0.026 longer and 0.05–0.09 Å longer, respectively, in **3**. Once again the longer distances in **3** are probably due to steric crowding.

There are two final aspects of the structure of $Zr_2H_4(BH_4)_4(dmpe)_2$ worth mentioning. First, as we have seen previously in other polynuclear zirconium hydrides, a highly asymmetric structure is adopted rather than the more symmetric structure that would result if the dmpe ligands were distributed equally among the two zirconium centers. This general pattern may be a consequence of the structural stability of the $Zr(BH_4)_3$ unit, which appears in all of the polynuclear hydrides we have prepared. Second, the ZrH_3Zr unit must also be a robust structural feature since it and the dinuclear structure are maintained even upon replacement of the unidentate PMe_3 groups with bidentate dmpe ligands.

Dynamic Behavior of the $M_2H_4(BH_4)_4(dmpe)_2$ Complexes. Of all the group 4 polyhydrides we have obtained to date by addition of phosphines to $M(BH_4)_4$, the only species which possesses both terminal and bridging hydrides are the two $M_2H_4(BH_4)_4(dmpe)_2$ complexes. At slightly elevated temperatures, the four hydrides in **3** undergo a terminal-bridging hydride exchange process that makes them all equivalent; in the same temperature range (20–40 °C), the ^{31}P NMR peaks coalesce. An activation barrier ΔG^* of 12.6 ± 0.1 kcal mol^{-1} can be calculated for this exchange process from the variable-temperature line shapes. Similar behavior is exhibited by the hafnium analogue **4** (Figures 8 and 9), and the activation barrier deduced is identical at 12.6 ± 0.1 kcal mol^{-1}. For this exchange process, we propose a mechanism that involves a "windshield-wiper" motion in which the terminal hydride moves into a bridging position as a briding hydride moves into the terminal position between the two dmpe ligands on the other side of the molecule. The process exchanges all the hydrides provided

that rotation of the Zr(μ-H)$_3$Zr unit about the Zr···Zr axis is fast. This dynamic process also accounts for the coalescence of the dmpe peaks in the $^{31}P\{^1H\}$ NMR spectrum since the A and B spins of the AA'BB' spin system are exchanged.

Exchange between terminal and bridging hydrogen atoms is usually not observable in group 4 polyhydrides. The cyclopentadienyl complexes $[Cp_2MH_2]_2$ and their ring-substituted analogues invariably exhibit distinct resonances for the two terminal and two bridging hydride ligands at all accessible temperatures.[18,27-29] Indirect evidence of exchange in the tetrahydroindenyl zirconium dihydride dimer was, however, obtained from a spin saturation transfer experiment at 30 °C.[26] In contrast, the analogous thorium complex $[Cp^*_2ThH_2]_2$, which also has two

(25) Fischer, M. B.; James, E. J.; McNeese, T. J.; Nyburg, S. C.; Posin, B.; Wong-Ng, W.; Wreford, S. S. *J. Am. Chem. Soc.* **1980**, *102*, 4941–4947.
(26) Wielstra, Y.; Meetsma, A.; Gambarotta, S. *Organometallics* **1989**, *8*, 258–259.
(27) Wailes, P. C.; Weigold, H.; Bell, A. P. *J. Organomet. Chem.* **1972**, *43*, C29–C31.
(28) Weigold, H.; Bell, A. P.; Willing, R. I. *J. Organomet. Chem.* **1974**, *73*, C23–C24.
(29) Courturier, S.; Tainturier, G.; Gautheron, B. *J. Organomet. Chem.* **1980**, *195*, 291–306.

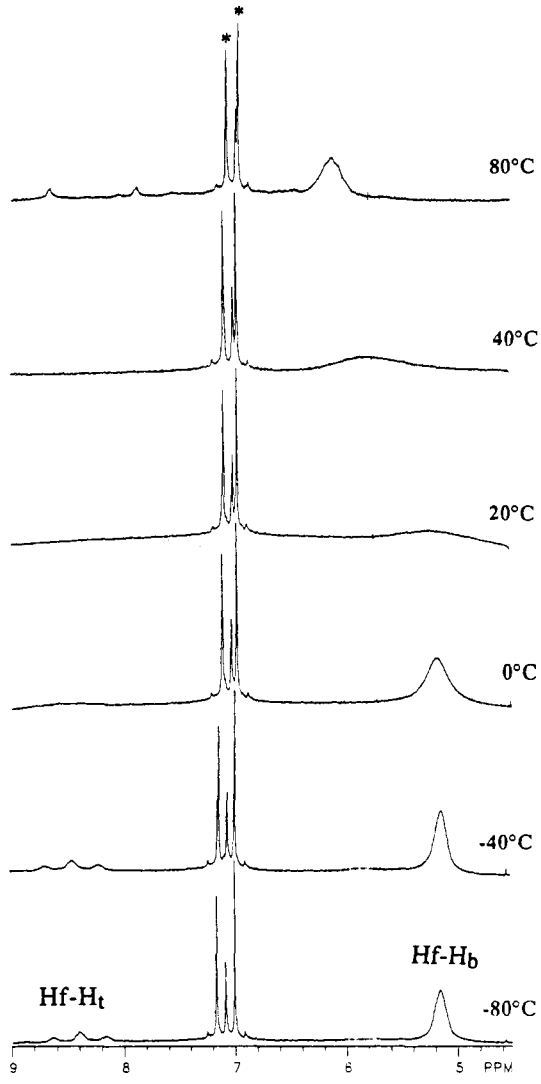

Figure 8. Variable-temperature 300-MHz ^1H NMR spectrum of $Hf_2H_4(BH_4)_4(dmpe)_2$, **4**, in C_7D_8. Some decomposition is evident at 80 °C.

terminal and two bridging hydride ligands, gives only one hydride resonance in its ^1H NMR spectrum even at −85 °C.[30,31]

Mechanistic Relationships between the Various Tetrahydroborate Complexes. We have attempted to obtain information about the mechanisms by which these group 4 hydrides are formed, and in particular to determine whether they are formed sequentially or independently from the $M(BH_4)_4$ starting materials. To this end, we have carried out in situ ^1H, ^{11}B, and ^{31}P NMR studies of the reactions of $M(BH_4)_4$ with PMe_3 and dmpe. These studies suggest that the various complexes *are* formed sequentially: $M(BH_4)_4 \rightarrow M_2H_3(BH_4)_5(PMe_3)_2 \rightarrow M_3H_6(BH_4)_6(PMe_3)_4$ and $M(BH_4)_4 \rightarrow MH(BH_4)_3(dmpe) \rightarrow MH_2(BH_4)_2(dmpe)_2 + M_2H_4(BH_4)_4(dmpe)_2$ in the sense that resonances due to these species appear in the order given. However, these results do *not* necessarily mean that one species is converted *directly* to the next in these sequences: various other resonances are also present at various times that presumably are due to hydride complexes that we have not been able to isolate. Unfortunately, the simultaneous existence of several species in solution has prevented us from establishing unambiguously the stoichiometries of these other species.

Complementary in situ NMR studies of the reactions of isolated samples of several of the new tetrahydroborate phosphine complexes have also been carried out. For example, heating a solution of $Hf_2H_3(BH_4)_5(PMe_3)_2$ and PMe_3 to 50 °C results in the partial conversion of this material to the trinuclear complex $Hf_3H_6(BH_4)_6(PMe_3)_4$. In contrast, addition of dmpe to $Zr_3H_6(BH_4)_6(PMe_3)_4$ gives the mononuclear species $ZrH_2(BH_4)_2(dmpe)_2$. These results suggest that the tetrahydroborate complexes can interconvert via multiple slow equilibria in solution. The relative concentrations of the various possible species appear to be dependent upon, inter alia, the reaction time, the temperature, the concentration of zirconium in solution, and the zirconium-to-phosphine ratio; we have not to date been able to make more definite conclusions about the mechanisms responsible for the formation and interconversion of these species.

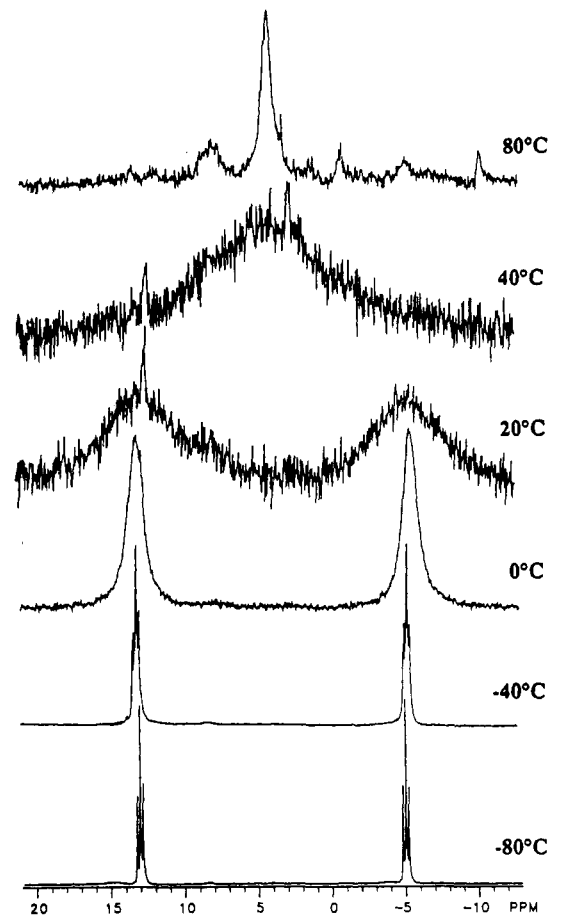

Figure 9. Variable-temperature 121.5-MHz $^{31}P\{^1H\}$ NMR spectrum of $Hf_2H_4(BH_4)_4(dmpe)_2$, **4**, in C_7D_8. Some decomposition is evident at 80 °C.

Concluding Remarks. We have isolated a series of new polyhydrides of zirconium and hafnium. The same reagents that yield $Zr_2H_3(BH_4)_5(PMe_3)_2$ and $Hf_2H_3(BH_4)_5(PMe_3)_2$[5] yield instead trinuclear species $Zr_3H_6(BH_4)_6(PMe_3)_4$ and $Hf_3H_6(BH_4)_6(PMe_3)_4$ when combined for longer reaction times. The trinuclear zirconium complex has been characterized crystallographically and the positions of the hydrides have been determined. So far, we have been unable to isolate mononuclear zirconium or hafnium hydrides by treatment of $Zr(BH_4)_4$ or $Hf(BH_4)_4$ with unidentate phosphines.

Like the dinuclear $M_2H_3(BH_4)_5(PMe_3)_2$ complexes, the trinuclear $M_3H_6(BH_4)_6(PMe_3)_4$ species engage in several dynamic exchange processes which we are unable to freeze out even at −80 °C. These exchange processes include interconversions between bidentate and tridentate BH_4^- groups, and apparent rotation of a $H_3Zr(BH_3)_3$ unit about a hydride-bridged Zr···Zr vector. In contrast to the behavior of some other polynuclear hafnium tetrahydroborates,[21] the BH_4^- groups do not exchange between metal centers. At higher temperatures, dissociation of the PMe_3 ligands becomes fast on the NMR time scale.

(30) Fagan, P. J.; Manriquez, J. M.; Maata, E. A.; Seyam, A. M.; Marks, T. J. *J. Am. Chem. Soc.* **1981**, *103*, 6650–6667.

(31) See also: Fendrick, C. M.; Schertz, L. D.; Day, V. W.; Marks, T. J. *Organometallics* **1988**, *7*, 1828–1838.

The zirconium and hafnium complexes of stoichiometry $M_2H_4(BH_4)_4(dmpe)_2$ can be prepared by addition of dmpe to $M_2H_3(BH_4)_5(PMe_3)_2$. Somewhat surprisingly, the dinuclear $M(\mu\text{-}H)_3M$ unit remains intact during this ligand substitution reaction despite the significantly different electronic and molecular structures characteristic of the two species. The single-crystal X-ray diffraction results for $Zr_3H_6(BH_4)_6(PMe_3)_4$ and $Zr_2H_4(BH_4)_4(dmpe)_2$ suggest that, in each molecule, three of the BH_4^- ligands are coordinated in a fashion that is intermediate between the η^2-BH_4^- and η^3-BH_4^- bonding modes.

Of all the group 4 polyhydrides that we have obtained by addition of phosphines to $Zr(BH_4)_4$, only $Zr_2H_4(BH_4)_4(dmpe)_2$, **3**, possesses both terminal and bridging hydrides. The four hydrides in **3** undergo a terminal-bridging hydride exchange, and a "windshield-wiper" motion of the set of four hydride ligands has been proposed to account for the exchange process. This dynamic process exchanges the chemically inequivalent nuclei and causes the dmpe peaks in the $^{31}P\{^1H\}$ NMR spectrum and the hydride peaks in the ^1H NMR spectrum to coalesce above 30 °C.

Finally, the isolation of zirconium and hafnium hydrides from the reactions of $Zr(BH_4)_4$ and $Hf(BH_4)_4$ with trialkylphosphines lends support to the suggestion that loss of BH_3 units from the $M(BH_4)_4$ precursors occurs under CVD conditions to give zirconium and hafnium hydrides that subsequently lose H_2. It is interesting to note that so far the minimum boron-to-metal ratio in these phosphine-stabilized complexes is 2:1; this ratio is present in the complexes $MH_2(BH_4)_2(dmpe)_2$, $M_2H_4(BH_4)_4(dmpe)_2$, and $M_3H_6(BH_4)_6(PMe_3)_4$ and is (coincidentally?) the same ratio as that present in the ceramic materials ZrB_2 and HfB_2.

Studies are underway to explore the catalytic or stoichiometric reactivity of these compounds and to determine whether they can serve as molecular precursors for metal boride phases.

Experimental Section

All operations were carried out in vacuum or under argon. Pentane and diethyl ether were distilled under nitrogen from sodium benzophenone immediately before use. Anhydrous $ZrCl_4$ and $HfCl_4$ were obtained from Cerac and were sublimed under vacuum; $LiBH_4$ (Strem) was used as received. Trimethylphosphine[32] and 1,2-bis(dimethylphosphino)ethane[33] were prepared by literature routes. The dinuclear zirconium and hafnium hydrides of stoichiometry $M_2H_3(BH_4)_5(PMe_3)_2$ were prepared as described previously.[5]

Despite many attempts, microanalyses of the zirconium and hafnium hydrides were always inaccurate and not reproducible; carbon analyses were usually low by two or more weight percentage units even in the presence of oxidation aids. Sample purity was accordingly established by NMR and IR spectroscopy. The IR spectra were recorded on a Perkin-Elmer 599B infrared spectrometer as Nujol mulls. The ^1H NMR data were obtained on a General Electric QE-300 spectrometer at 300 MHz or a General Electric GN-500 spectrometer at 500 MHz. The ^{11}B and ^{31}P NMR data were recorded on a GN-300 NB spectrometer at 96.25 and 121.44 MHz, respectively, or on the GN-500 spectrometer at 160.44 and 202.44 MHz. Chemical shifts were measured using internal standards and are reported in δ units (positive shifts to high frequency) relative to $SiMe_4$ (^1H), $BF_3{\cdot}Et_2O$ (^{11}B), or 85% H_3PO_4 (^{31}P). The intramolecular exchange rates used to determine the activation energies for fluxional processes were obtained from fits of the observed line shapes to those calculated for a two-site exchange.

Hexakis(μ-hydrido)hexakis(tetrahydroborato)tetrakis(trimethylphosphine)trizirconium(IV), 1. To $ZrCl_4$ (1.00 g, 4.29 mmol) and $LiBH_4$ (0.90 g, 41.32 mmol) was added diethyl ether (40 mL), and the white mixture was stirred at 25 °C for 5 min. The volatile components, diethyl ether and $Zr(BH_4)_4$, were distilled under vacuum from the room temperature reaction flask into a receiver cooled to −196 °C. The distillate was warmed to −78 °C and treated with PMe_3 (1.42 mL, 14.0 mmol) to give a milky white mixture. The solution was stirred for 15 min at −78 °C and then warmed to 25 °C. During this time, the color of the solution progressed through colorless, yellow, amber, olive green, and deep burgundy stages. At the end of this sequence (ca. 15 min), some green precipitate had formed. The solution was stirred for 5 h at 25 °C and then the solvent was removed under vacuum. The $H_3B{\cdot}PMe_3$ was removed at 25 °C by sublimation onto a cold finger cooled to −78 °C. The nonvolatile residue was washed with pentane (2 × 20 mL) and extracted with toluene (25 mL) to give a burgundy-colored solution. The filtered extract was concentrated to ca. 5 mL and cooled to −20 °C to give a red-brown solid, which was collected by filtration. Recrystallization of the crude reddish-brown product from toluene (5 mL) at −20 °C gave colorless crystals of the product suitable for X-ray diffraction. Yield: 0.25 g (26%). Mp: 140 °C dec. IR (cm^{-1}): 2530 m, 2495 s, 2430 m, 2400 s, 2385 sh, 2320 sh, 2230 w, 2135 s, 2095 s, 1420 w, 1375 w, 1300 w, 1240 w, 1185 w, 1160 vw, 1120 m, 1085 sh, 1005 vw, 945 s, 840 w, 830 sh, 780 sh, 770 w, 660 w.

Hexakis(μ-hydrido)hexakis(tetrahydroborato)tetrakis(trimethylphosphine)trihafnium(IV), 2. To $HfCl_4$ (0.85 g, 2.65 mmol) and $LiBH_4$ (0.80 g, 36.7 mmol) was added diethyl ether (40 mL), and the white mixture was stirred at 25 °C for 5 min. The volatile components, diethyl ether and $Hf(BH_4)_4$, were distilled under vacuum from the room temperature reaction flask to a receiver cooled to −196 °C. The distillate was warmed to −78 °C and treated with PMe_3 (1.21 mL, 11.9 mmol) to give a milky white mixture. The solution was stirred for 15 min at −78 °C and then warmed to 25 °C. A brown solution and a tan precipitate formed after the solution had been stirred for 12 h at 25 °C. The solvent was removed under vacuum, and the $H_3B{\cdot}PMe_3$ was removed at 25 °C by sublimation onto a cold finger cooled to −78 °C. The nonvolatile residue was washed with pentane (2 × 20 mL) and extracted with toluene (25 mL) to give an orange-red solution. The filtered extract was concentrated to ca. 5 mL and cooled to −20 °C to give the off-white microcrystalline product. Yield: 0.19 g (23%). Mp: 125–127 °C dec. IR (cm^{-1}): 2535 m, 2500 s, 2435 m, 2400 s, 2235 w, 2150 s, 2100 s, 1510 m br, 1465 w, 1375 w, 1300 w, 1285 w, 1255 vw, 1195 vw, 1160 vw br, 1125 m, 945 s, 845 w, 800 m, 750 vw, 665 w.

Hydridotris(μ-hydrido)tetrakis(tetrahydroborato)bis(1,2-bis(dimethylphosphino)ethane)dizirconium(IV), 3. To $Zr_2H_3(BH_4)_5(PMe_3)_2$ (0.54 g, 1.31 mmol) was added pentane (200 mL). The solution was cooled to 0 °C and treated with dmpe (1.0 mL, 6.0 mmol), and the mixture immediately become cloudy white. The solution turned red-pink after being stirred for a few minutes. The solution was allowed to stir at 0 °C for 1.5 h, and then the pink precipitate was collected by filtration. The solid was extracted twice with Et_2O (100 mL + 50 mL) at 0 °C. The orange-red extracts were combined, filtered, concentrated to ca. 50 mL, and cooled to −20 °C to give colorless crystals of the product. Yield: 0.27 g (42%). Mp: 185 °C dec. IR (cm^{-1}): 2490 s, 2370 m, 2300 m br, 2200 m br, 2175 m, 2140 w sh, 2110 vw, 1510 m, 1430 vw sh, 1419 w, 1410 vw sh, 1365 w, 1300 vw, 1285 vw, 1278 vw, 1235 vw br, 1183 w br, 1150 w, 1125 vw, 1102 m, 1059 vw, 1025 vw, 990 vw, 941 s, 925 s, 888 w, 861 vw, 832 w, 801 w, 785 vw br, 760 vw, 700 m, 628 w.

Hydridotris(μ-hydrido)tetrakis(tetrahydroborato)bis(1,2-bis(dimethylphosphino)ethane)dihafnium(IV), 4. This compound was prepared as for the zirconium analogue from $Hf_2H_3(BH_4)_5(PMe_3)_2$ (0.95 g, 1.62 mmol) and dmpe (1.1 mL, 6.5 mmol) in pentane (200 mL) at 0 °C to give a yellow solution which was allowed to stir for 4 h. The off-white precipitate was collected by filtration and extracted twice with Et_2O (200 mL + 100 mL) at 0 °C. The pale yellow extracts were combined, filtered, concentrated to ca. 100 mL, and cooled to −20 °C to afford colorless crystals. Yield: 0.50 g (43%). Mp: 200 °C dec. IR (cm^{-1}): 2490 m, 2370 m, 2300 w br, 2200 w br, 2175 w, 2110 vw br, 1545 w br, 1430 vw sh, 1420 vw, 1410 vw sh, 1365 w sh, 1305 vw, 1288 vw, 1280 vw, 1155 w br, 1105 m, 1060 vw, 1030 vw, 990 vw, 945 m, 927 m, 891 w, 862 vw, 852 vw br, 845 vw br, 835 w, 705 w, 638 w.

Crystallographic Studies.[34] Single crystals of $Zr_3H_6(BH_4)_6(PMe_3)_4$, **1**, grown from toluene, were mounted on glass fibers with Paratone-N oil (Exxon) and were quickly cooled to −75 °C in a cold nitrogen gas stream on the diffractometer. [Crystals of $Zr_2H_4(BH_4)_4(dmpe)_2$, **3**, were grown from diethyl ether and mounted similarly on the diffractometer. Subsequent comments in brackets will refer to this compound.] The crystal chosen had a narrow (ca. 0.2°) ω-scan but was apparently twinned and gave a broad mosaic spread. Examination under plane polarized light showed that the twinning was not significant, and no problems were encountered during data collection. [Crystals of **3** showed no evidence of twinning.] Standard peak search and indexing procedures gave rough cell dimensions, and the diffraction symmetry was supported by examination of axial photographs. Least-squares refinement using 25 reflections yielded the cell dimensions given in Table II.

Data were collected in one quadrant of reciprocal space ($+h,+k,\pm l$) by using measurement parameters listed in Table II. [For compound **3**, one quadrant ($+h,\pm k,+l$) of data was collected over the range $2.0 < 2\theta < 54$ °, and a complete set of intensities ($\pm h,\pm k,\pm l$) was collected over

(32) Luetkens, M. L.; Sattelberger, A. P.; Murray, H. H.; Basil, J. D.; Fackler, J. P. *Inorg. Synth.* **1989**, *26*, 7–12.

(33) Henderson, R. A.; Hussain, W.; Leigh, G. J.; Normanton, F. B. *Inorg. Synth.* **1985**, *23*, 141–143.

(34) For details of the crystallographic procedures used, see: Jensen, J. A.; Wilson, S. R.; Girolami, G. S. *J. Am. Chem. Soc.* **1988**, *110*, 4977–4982.

(35) Infrared stretches for terminal Zr–H bonds can lie below 1500 cm^{-1}; see: Gell, K. I.; Schwartz, J. *Inorg. Chem.* **1980**, *19*, 3207–3211.

a limited 2θ range between 2.0 and 12.0°.] Systematic absences for $h0l$ ($h + l \neq 2n$) and $0k0$ ($k \neq 2n$) were consistent only with space group $P2_1/n$. [For 3, the systematic absences $0kl$ ($k + l \neq 2n$) and $0hl$ ($h \neq 2n$) were consistent with space groups $Pna2_1$ and $Pnam$. The acentric space group was established from the average values of the normalized structure factors, the successful refinement of the proposed model in the acentric space group, and the orientation of the molecule with respect to the c-axis.] The measured intensities were reduced to structure factor amplitudes and their esd's by correction for background, scan speed, and Lorentz and polarization effects. While corrections for crystal decay were unnecessary, absorption corrections were applied, the maximum and minimum transmission factors being 0.837 and 0.731. [For 3, the absorption correction was complicated due to the difficulty of indexing the faces. The maximum and minimum transmission factors were 0.867 and 0.826, respectively.] Systematically absent reflections were deleted, and symmetry equivalent reflections were averaged to yield the set of unique data. Only those data with $I > 2.58\sigma(I)$ were used in the least-squares refinement.

The structure was solved using direct methods (SHELXS-86). The positions of the zirconium and phosphorus atoms were deduced from an E-map [for 3, only the zirconium atoms were located initially]. Subsequent least-squares refinement and difference Fourier syntheses revealed the positions of the remaining atoms. The quantity minimized by the least-squares program was $\sum w(|F_o| - |F_c|)^2$, where $w = 1.21/(\sigma(F_o)^2 + (pF_o)^2)$ [for 3, $w = 1.04/(\sigma(F_o)^2 + (pF_o)^2)$]. The analytical approximations to the scattering factors were used, and all structure factors were corrected for both the real and imaginary components of anomalous dispersion. In the final cycle of least squares, all non-hydrogen atoms were independently refined with anisotropic thermal coefficients, and a group isotropic thermal parameter was varied for the hydrogen atoms. The hydrogen atoms were located in the Fourier difference maps, and their locations were independently refined with isotropic thermal parameters. [For 3, anisotropic thermal parameters were refined for the zirconium, phosphorus, and carbon atoms, and isotropic thermal parameters were varied for the boron atoms. Most of the hydrogen atoms appeared in the difference Fourier maps. In the final model, the aliphatic hydrogen atoms were included as fixed contributors in "idealized" positions with C-H = 0.95 Å. In contrast, the positions of hydrogen atoms attached to zirconium and in the BH_4 groups were independently refined. A common isotropic thermal parameter was varied for all the hydrogen atoms.] An isotropic extinction parameter was also refined, which converged to 2.2 (3) $\times 10^{-8}$ [for 3, 3.5 (3) $\times 10^{-8}$]. Successful convergence was indicated by the maximum shift/error of 0.005 [for 3, 0.003] in the last cycle. Final refinement parameters are given in Table II. The final difference Fourier map had no significant features. There were no apparent systematic errors among the final observed and calculated structure factors.

Acknowledgment. We thank the Department of Energy (Grant DE-AC02-76ER-01198) for support of this work. We thank Charlotte Stern of the University of Illinois X-ray Crystallographic Laboratory for assisting with the crystal structure determinations and Yujian You for carrying out one NMR study. G.S.G. is the recipient of a Henry and Camille Dreyfus Teacher-Scholar Award (1988-1993).

Supplementary Material Available: Tables of atomic coordinates, thermal parameters, and bond distances and angles for $Zr_3H_6(BH_4)_6(PMe_3)_4$ and $Zr_2H_4(BH_4)_4(dmpe)_2$ and calculated hydrogen atom positions for $Zr_2H_4(BH_4)_4(dmpe)_2$ (15 pages); tables of final observed and calculated structure factors for $Zr_3H_6(BH_4)_6(PMe_3)_4$ and $Zr_2H_4(BH_4)_4(dmpe)_2$ (31 pages). Ordering information is given on any current masthead page.

Efficient Transfer-Dehydrogenation of Alkanes Catalyzed by Rhodium Trimethylphosphine Complexes under Dihydrogen Atmosphere

John A. Maguire, Angelo Petrillo, and Alan S. Goldman*

Contribution from the Department of Chemistry, Rutgers, The State University of New Jersey, New Brunswick, New Jersey 08903. *Received June 17, 1992. Revised Manuscript Received July 31, 1992*

Abstract: $RhL_2Cl(CO)$ (1; L = PMe_3), a known catalyst for the photodehydrogenation of alkanes, is found to catalyze the highly efficient thermal (nonphotochemical) transfer-dehydrogenation of alkanes under high-pressure hydrogen atmosphere. The proposed mechanism involves addition of H_2, loss of CO, and transfer of H_2 to a sacrificial acceptor, thereby generating RhL_2Cl, the same catalytically active fragment formed by photolysis of 1. Consistent with this proposal, we report that photochemically inactive species, RhL_2ClL' (L' = $PiPr_3$, PCy_3, PMe_3) and $[RhL_2Cl]_2$, are also thermochemical catalyst precursors. These species demonstrate much greater catalytic activity than $RhL_2Cl(CO)$, particularly under moderate hydrogen pressures (ca. 500 times greater under 800 Torr of H_2 at 50 °C). The dependence of the turnover rates on hydrogen pressure is consistent with the proposed role of hydrogen, i.e., displacement of L' from the four-coordinate complexes or fragmentation of $H_2Rh_2L_4Cl_2$, giving H_2RhL_2Cl, which is dehydrogenated by olefin to give RhL_2Cl. Selectivity studies provide further support for the characterization of the active fragment.

The catalytic functionalization of alkanes is currently one of the major challenges of organometallic chemistry.[1,2] Dehydrogenation to give alkenes is one potential functionalization that is attractive in view of the versatility of alkenes as precursors for a wide range of useful and facile transformations. The ability of organometallic complexes to catalyze alkene hydrogenation with remarkable effectiveness[3] is promising in the context of dehydrogenation. Indeed, alkane transfer-dehydrogenation systems (i.e., systems using a sacrificial hydrogen acceptor), first developed by Crabtree and Felkin, have long stood as the foremost examples of organometallic-catalyzed alkane functionalization.[4,5] However,

* To whom correspondence should be addressed at the Department of Chemistry, Rutgers University Piscataway, NJ 08855-0939.

(1) For reviews of alkane C-H bond activation by organometallic complexes see: (a) Bergman, R. G. *Science (Washington, D.C.)* **1984**, *223*, 902. (b) Janowicz, A. H.; Periana, R. A.; Buchanan, J. M.; Kovac, C. A.; Stryker, J. M.; Wax, M. J.; Bergman, R. G. *Pure Appl. Chem.* **1984**, *56*, 13-23. (c) Crabtree, R. H. *Chem. Rev.* **1985**, *85*, 245. (d) Halpern, J. *Inorg. Chim. Acta* **1985**, *100*, 41-48. (e) Jones, W. D.; Feher, F. J. *Acc. Chem. Res.* **1989**, *22*, 91 and ref 2.

(2) For a general review of homogeneous alkane functionalization with an emphasis on catalysis see: *Activation and Functionalization of Alkanes*; Hill, C., Ed.; John Wiley & Sons: New York, 1989.

0002-7863/92/1514-9492$03.00/0